# A NUMERICAL EXPERIMENT ON SCREENING OF SURFACE WAVE AT AN OPEN TRENCH

by

Naoto OHBO[I] and Tsuneo KATAYAMA[II]

SYNOPSIS

Numerical simulation was made to determine the effect of an open trench on the *Rayleigh* wave propagation. The *Rayleigh* wave was generated in this study by one cycle normal force applied at the free surface of the two-dimensional homogeneous elastic medium with the Poisson's ratio of $\nu=0.25$. From the numerical experiment, it was found that a converted *P* wave is generated at a trench when the propagating wave goes across it. This converted *P* wave was found to greatly influence the horizontal component of the ground motion near the trench. Far from the trench, however, *Rayleigh* wave dominates both in the vertical and the horizontal motions. The transmission coefficient $T$ determined from the computed results in the far field was found to be expressed by an equation $T=\exp(-2D)$, where $D$ is the ratio of trench depth to *Rayleigh* wave-length.

## INTRODUCTION

Wave propagation in an elastic medium has been studied by a number of reseachers for a long time, both analytically and numerically. The propagation of impulsive elastic wave excited by line or point source in elastic half-space medium with a free surface boundary was first examined by H. Lamb in his wellknown paper[1].

To minimize the effect of propagation wave on a structure or to reduce the energy emitted from a vibrating structure, structures are often recommended to be isolated from the surrounding soil. An open trench, sheet-piling and other similar methods are used for this purpose. However, there seems to be a general agreement that construction of an open trench around the source of vibration is one of the most effective methods.

Earlier studies have shown that the effect of screening is generally influenced by the trench depth, and that the effectiveness of an open trench is related to the ratios of trench depth and trench width to the incident *Rayleigh* wave-length[2-6]. In spite of some recent developments[7-12], theoretical results are generally difficult to apply for practical situations because of the nonuniformity of media and complicated geometrical configuration. Therefore, the characteristics of the complex transmission, reflection and refraction of body and *Rayleigh* waves at an open trench have not been well understood today.

In this paper, the characteristics of the wave screening and propagation at an open trench were investigated in detail by using the numerical method proposed by Y. Satô[13]. In the following sections, the numerical method and some typical results of analysis are presented.

---

I) Research Associate, II) Associate Professor, Institute of Industrial Science, University of Tokyo

NUMERICAL METHOD AND COMPUTATIONAL DETAIL

*EQUATION OF MOTION:* Let $x$ and $z$ be the horizontal and vertical coordinates in a two-dimensional elastic half-space, and let the positive direction of $z$-axis be downward. The equations of motion in the elastic medium are given by

$$\rho\frac{\partial^2 u}{\partial t^2} = (\lambda+\mu)\frac{\partial^2 u}{\partial x^2} + \mu\nabla^2 u + (\lambda+\mu)\frac{\partial^2 w}{\partial x \partial z}$$
$$\rho\frac{\partial^2 w}{\partial t^2} = (\lambda+\mu)\frac{\partial^2 w}{\partial z^2} + \mu\nabla^2 w + (\lambda+\mu)\frac{\partial^2 u}{\partial x \partial z} \qquad (1)$$

where $u$ and $w$ are the displacements in the $x$ and $z$ directions, respectively, $\rho$ is the density, $t$ is the time, and $\lambda$ and $\mu$ are the Lamé's constants.

Boundary conditions for the problem are determined by the fact that the normal and tangential stresses must vanish on the free surface. Normal and tangential stresses can be expressed in terms of the displacement components as

$$\sigma_{zz} = \lambda\frac{\partial u}{\partial x} + (\lambda+\mu)\frac{\partial w}{\partial z}$$
$$\sigma_{xx} = \lambda\frac{\partial w}{\partial z} + (\lambda+\mu)\frac{\partial u}{\partial x}$$
$$\tau_{xz} = \mu\left(\frac{\partial u}{\partial z} + \frac{\partial w}{\partial x}\right) \qquad (2)$$

Hence the boundary conditions at the free surface are given by $\sigma_{zz}=0$ and $\tau_{xz}=0$ at $z=0$.

Wave propagation is analyzed by solving Eqs. (1) and (2) by replacing the various derivatives by their central difference approximations. In this method, however, difficulty arises in the approximation of the conditions to be satisfied at a corner point. Moreover there is a restriction on the value of the Poisson's ratio to be used and the stability of computation is lost near the boundary if this restriction is not observed[14].

*METHOD PROPOSED BY Y. SATÔ*[13]*:* Assume a two-dimensional framework of a mass-spring system as shown in Fig. 1. The point $(i,j)$ is connected by springs to the neighbouring points. Here $i$ and $j$ are the indices along the $x$ and $z$ directions, respectively. The equation of motion of the mass $m$ in the $x$ direction at point $(i,j)$ is given by

$$m\frac{d^2 u}{dt^2} = C_1\cdot(u_{i+1,j} + u_{i-1,j} - 2u_{i,j})$$
$$+ (C_2/2)(u_{i+1,j+1} + u_{i+1,j-1} + u_{i-1,j+1} + u_{i-1,j-1} - 4u_{i,j})$$
$$+ (C_2/2)(w_{i+1,j+1} - w_{i+1,j-1} - w_{i-1,j+1} + w_{i-1,j-1}) \qquad (3)$$

where $C_1$ is the spring constant along the $x$ or $z$ coordinate axis, and $C_2$ is that in the diagonal direction. A similar equation may be obtained for the $z$-direction.

Using the central difference formula, the terms in the parenthese in

the right hand side of Eqs. (3) can be written as

$$u_{i+1,j} + u_{i-1,j} - 2u_{i,j} = h^2 \frac{d^2 u}{dx^2}$$

$$u_{i+1,j+1} + u_{i+1,j-1} + u_{i-1,j+1} + u_{i-1,j-1} - 4u_{i,j} = 2h^2 \left(\frac{d^2}{dx^2} + \frac{d^2}{dz^2}\right) u$$

$$= 2h^2 \nabla^2 u$$

$$w_{i+1,j+1} - w_{i+1,j-1} - w_{I-1,j+1} + w_{i-1,j-1} = 4h^2 \frac{d^2 w}{dx dz}$$

By introducing

$$m = \rho h^2$$

into the left hand side of Eqs. (3) the following equation is obtained

$$\rho \frac{d^2 u}{dt^2} = C_1 \frac{d^2 u}{dx^2} + C_2 \nabla^2 u + 2C_2 \frac{d^2 w}{dx dz} \tag{4}$$

which is equivalent to Eqs. (1) when $C_1 = \lambda + \mu$ and $C_2 = \mu$, if and only if $\lambda = \mu$.

The boundary conditions at the free surface and corner are also given by Satô[13].

*COMPUTATIONAL DETAIL:* The model is two-dimensional and has the axial symmetry with the $z$ axis (see Fig.2). It is assumed in this paper that $P$ and $S$ wave velocities ($V_P$ and $V_S$) are 200 m/s and 115.5 m/s, respectively. Therefore, the Poisson's ratio is 0.25 and the *Rayleigh* wave velocity $V_R$ is 106 m/s. The grid spacing $h$ was assumed to be 1 m and the time increment of $\Delta t = 0.00433$s was used.

The exciting normal force applied on the free surface at $z=0$ was

$$P(t,x) = F(t) \cdot G(x)$$

where

$$F(t) = \begin{cases} \sin(2\pi f t) & 0 \le t \le 1/f \\ 0 & 1/f < t \end{cases}$$

and

$$G(x) = \begin{cases} (1+\cos(\pi f x / V_S))/2 & 0 \le x \le 2f/V_S \\ 0 & 2f/V_S < x \end{cases}$$

where $F(t)$ and $G(x)$ are the time and space functions, and $f$ is the frequency. The wave-length of the *Rayleigh* wave generated by this force is estimated as about 10m.

The configuration of the models and the notations used in this analysis are shown in Fig. 2.

## WAVE PROPAGATION CHARACTERISTICS

*HALF-SPACE MODEL:* This simple case was analyzed to examine the validity and accuracy of the numerical method. Figure 3 shows the wave propagation pattern in the form of the two-dimensional displacement field at $t=70\cdot\Delta t$, which clearly indicates the propagations of the two body waves (the compressional, *P*, and the shear, *S*) and one surface wave (the *Rayleigh* wave, *R*). The geometrical damping laws for the body and *Rayleigh* wave obtained from the analysis were $r^{-1/2}$ and $r^{-0}$, which were in accordance with the results of the two-dimensional theoretical analysis. The wave propagation pattern such as the one shown in Fig. 3 is most effective in providing the macroscopic visualization of wave phenomena.

The particle motion obtained at the point $r=37$ m is shown in Fig. 4. This motion indicates a retrograde ellipse and infers the *Rayleigh* wave propagating along the free surface of the elastic medium.

The wave forms observed at several points located along the surface are shows in Fig. 5. The amplitude scale is arbitrary except for the fact that the ratio between the horizontal and vertical amplitudes is correct. The upward and downward arrows in Fig. 5 indicate the *P* and *Rayleigh* phases, respectively. The velocities of *P*, *S* and *Rayleigh* waves determined from the analysis were 200 m/s, 116 m/s and 106 m/s, respectively.

*OPEN TRENCH MODEL (L=3, D=0.6):* Figure 6 shows the wave propagation pattern at $t=85\cdot\Delta t$.

The displacement-time history observed at several points on the free surface are shown in Fig. 7. In comparison with the ones without a trench (Fig. 5), a secondary wave appears between the direct *P* and *Rayleigh* wave, which also propagates with the velocity of the *P* wave. This is the converted *P* wave. The horizontal displacement due to the converted *P* wave is large near the trench, however, it becomes smaller as the distance from the trench increases. The effect of the converted *P* wave on the vertical displacement is small near the trench, but it becomes more recognizable at the distance with several wave-lengths from the trench.

The wave forms observed at several depths at the point $r=70$ m distant from the source (30 m from the trench) are shown in Fig. 8. The arrows indicate the arrivals of the *P* and *Rayleigh* waves. The *Rayleigh* wave amplitude is found to decrease rapidly with depth. On the other hand the *P* wave amplitude is almost independent of the depth of observation. This difference was noted even near the trench

## SCREENING EFFECT OF TRENCH

*THEORETICAL APPROACH:* At the trench, the incident *Rayleigh* wave may be partitioned into the following two parts, (1) the reflected *Rayleigh* wave, and (2) the transmitted *Rayleigh* wave, as shown Fig. 9. $E_i$, $E_r$ and $E_t$ are the energy distributions of the incident, reflected and transmitted *Rayleigh* waves, respectively. Therefore, the conservation of energy at the trench may be expressed as

$$E_i = E_r + E_t \tag{5}$$

The kinetic energies of the three types of waves are expressed as follows

$$E_i = \rho\omega^2 \int_0^{\infty} \{\dot{u}(\omega)^2 + \dot{w}(\omega)^2\} dD \tag{6}$$

$$E_r = \rho\omega^2 \int_0^{D_i} \{\dot{u}(\omega)^2 + \dot{w}(\omega)^2\} dD \tag{7}$$

$$E_t = \rho\omega^2 \int_{D_i}^{\infty} \{\dot{u}(\omega)^2 + \dot{w}(\omega)^2\} dD \tag{8}$$

where $\rho$ is the density, $\omega$ is the angular frequency, and $\dot{u}(\omega)$ and $\dot{w}(\omega)$ are the horizontal and vertical velocity amplitude, respectively.

The energy of the transmitted *Rayleigh* can be calculated from Eqs. (8) because the transmitted *Rayleigh* wave should not exist behind the trench. Since *Rayleigh* wave usually develops after having travelled a distance of several wave-lengths, the horizontal and vertical components of the developed *Rayleigh* waves, $u_d$ and $w_d$, to be observed at a point more than 30 m distant from the trench may be expressed as follows

$$u_d(\omega) = T \cdot u(\omega), \qquad w_d(\omega) = T \cdot w(\omega) \tag{9}$$

where $T$ is the coefficient of transmission of the *Rayleigh* wave.
The kinetic energy of the developed *Rayleigh* wave $E_d$ may be evaluated by

$$E_d = \rho\omega^2 \int_0^{\infty} \{\dot{u}_d(\omega)^2 + \dot{w}_d(\omega)^2\} dD \tag{10}$$

Substituting Eqs. (9) into (10) gives

$$E_d = T^2 \cdot \rho\omega^2 \int_0^{\infty} \{\dot{u}(\omega)^2 + \dot{w}(\omega)^2\} dD \tag{11}$$

If this energy $E_d$ is equated with the transmitted energy $E_t$, we have

$$\rho\omega^2 \int_{D_i}^{\infty} \{\dot{u}(\omega)^2 + \dot{w}(\omega)^2\} dD = T^2 \cdot \rho\omega^2 \int_0^{\infty} \{\dot{u}(\omega)^2 + \dot{w}(\omega)^2\} dD \tag{12}$$

from which

$$T = \left\{ \frac{\int_{D_i}^{\infty} \{\dot{u}(\omega)^2 + \dot{w}(\omega)^2\} dD}{\int_0^{\infty} \{\dot{u}(\omega)^2 + \dot{w}(\omega)^2\} dD} \right\}^{1/2} \tag{13}$$

The transmission coefficients may be evaluated for different values of depth $D_i$ in Eqs. (13).

*RESULTS OF NUMERICAL EXPERIMENT:* The transmission coefficient $T$ is obtained by the ratio between the calculated *Rayleigh* wave amplitudes $A_o$ and $A_t$, where $A_t$ is the maximum amplitude observed far from the trench for the trench model and $A_o$ is that at the same point for the no-trench model. There are two kinds of the transmission coefficients: one from the horizontal component of *Rayleigh* wave displacement, and another from the vertical component. These values must be equal to one another.

In the case of the trench model with $L$=3 and $D$=0.6, the transmission coefficients for the vertical and horizontal components obtained from the analysis are plotted in Fig. 10. It is noticed that the largest value of coefficient for the horizontal component occurs near the trench, while the coefficient for the vertical component is almost independent of the distance

from the trench. The two coefficients become almost equal at points farther than 30 m apart from the trench. The former phenomenon is due to the fact that the horizontal displacement of the transmitted wave near the trench strongly contains the effect of the converted $P$ wave.

Figure 11 shows the relation of the transmission coefficients obtained at 30 m and 35 m distant from the trench with the ratio of the trench depth to the *Rayleigh* wave-length, $D$. The transmission coefficient decreases as the trench depth increases. The solid and dashed lines indicate the regression lines obtained from this study and the theoretical curve discussed in the proceeding section, respectively. The data points in Fig. 11 are obtained for two different trench positions, namely $L$=2 and 4. It is seem that the transmission coefficients decrease almost exponentially with $D$. Moreover, this regression line was found to hold for the two different trench positions.

## CONCLUSIONS

In this paper, we dealt with the wave propagation in the elastic half-sapce due to a normal force applied on its free surface and the screening effect of an open trench by way of a numerical study. Major points of interest found from the study are summarized below:

(1) A new type of wave was found to be generated when wave propagates across an open trench. From its propagation velocity, this wave was found to be a converted $P$ wave.

(2) The effect of the converted $P$ wave is large for the horizontal motion near the trench, while the motion at the locations sufficiently far from the trench is mostly governed by the *Rayleigh* wave.

(3) The transmission coefficient across the trench, $T$, may be described by

$$T = \exp(-2D) \quad \text{for } D \leq 0.8$$

where $D$ is the ratio of the trench depth to the wave-length of the *Rayleigh* wave.

## ACKNOWLEDGMENTS

The authors wish to express their gratitude for the guidance and encouragement recieved from Prof. K. Kubo, University of Tokyo, Dr. I. Onda, Gunma University, and Prof. Y. Satô, Kagoshima University. The numerical computations in this study were performed on the HITACHI M-200H at the Data Processing Center, University of Tokyo. The financial support provided by Grant-in-Aid for Encouragement of Young Scientist (56750300) is acknowleged.

## REFERENCES

[1] H. Lamb (1904), "On the propagation of Tremors Over the Surface of an Elastic Solod", Philosophical Transactions, Royal Society, London, Series A, Vol.203.

[2] T. Terada and C. Tsuboi (1927), "Experimental Studies on Elastic Wave, Part 1", Bull. Earthq. Res. Inst., Univ. of Tokyo, Vol.3, No.1.

[3] C. Tsuboi (1928), "Experimental Studies on Elastic Wave, Part 2", Bull. Earthq. Res. Inst., Univ. of Tokyo, Vol.4, No.1.

[4] Z. Suzuki and A. Ishigaki (1958), "On the Shielding Effect of Various Types of Canals (in Japanese)", Jour. Seism. Soc. Japan., Vol.11, No.1.
[5] Z. Suzuki and A. Ishigaki (1959), "On Converted Waves by a Narrow Canal on the Surface of a Semi-Infinite Elastic Medium", Sci. Rep., Tohoku Univ., Series 5, Vol.10.
[6] T. Yoshii (1971), "Attenuation of Rayleigh Waves Caused by a Narrow Trench (in Japanese)", Jour. Seism. Soc. Japan, Vol.33, No.1.
[7] K. Fujii, Y.Nakayama, K. Imai and M. Nakano (1980), "Group of Rayleigh Waves Transmitted Across a Trench on the Surface of Elastic Half-Space (I) (in Japanese)", Jour. Seism. Soc. Japan, Vol.33, No.1.
[8] K. Fujii, T. Takimoto, Y. Nakayama and M. Nakano (1980), "Group of Rayleigh Waves Transmitted Across a Trench on the Surface of Elastic Half-Space (II) (in Japanese)", Jour. Seism. Soc. Japan, Vol.33, No.1.
[9] R. D. Wood (1968), "Screening of Surface Waves in Soils", Jour. Soil Mech. and Found. Div., Proc. ASCE, Vol.84, No.SM4.
[10] M. Fuyuki and Y. Matsumoto (1980), "Finite Difference Analysis of Rayleigh Wave Scattering at a Trench", Bull. Seis. Soc. Amer., Vol.70, No.6.
[11] N. Ohbo and T. Katayama (1981), "Elastic Wave Propagation in Elastic Medium with a Trench (in Japanese)", "SEISAN-KENKYU", Jour. Inst. Indus. Sci., Univ. of Tokyo, Vol.33, No.3.
[12] N. Ohbo and T. Katayama (1981), "Screening of Elastic Wave with Trench in Elastic Medium (in Japanese)", "SEISAN-KENKYU", Jour. Inst. Indus. Sci., Univ. of Tokyo, Vol.33, No.5.
[13] Y. Satô (1972), "A Numerical Experiment on Wave Propagation in an Elastic Quarter Space", Jour. Phy. Earth., Vol.21, No.1.
[14] A. Ilan and D. Loewenthal (1976), "Instability of Finite Difference Scheme due to Boundary Conditions in Elastic Media", Geophy. Prospect., Vol.24.

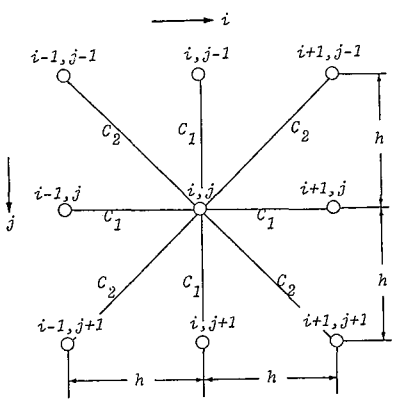


Fig.1. Mass-Spring System

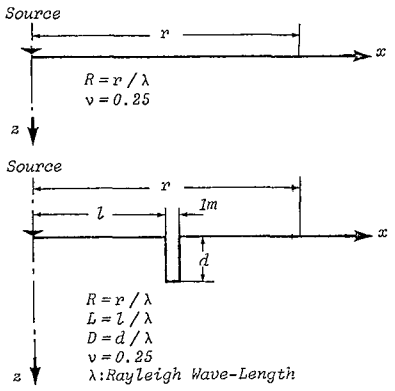


Fig.2. Two-Dimensional Configuration of the Half-Space and the Trench Models

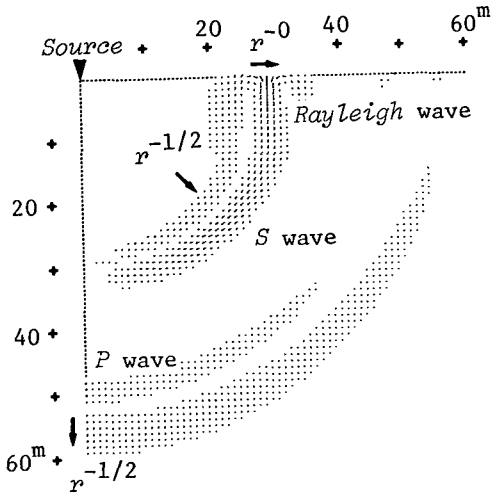


Fig.3. Displacement Vector Field in the Elastic Half-Space Model at $t=70\cdot\Delta t$

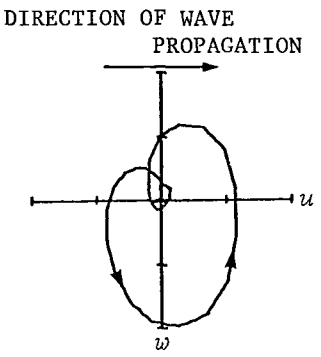


Fig.4. Particle Motion on the Free Surface at $r$=37 m

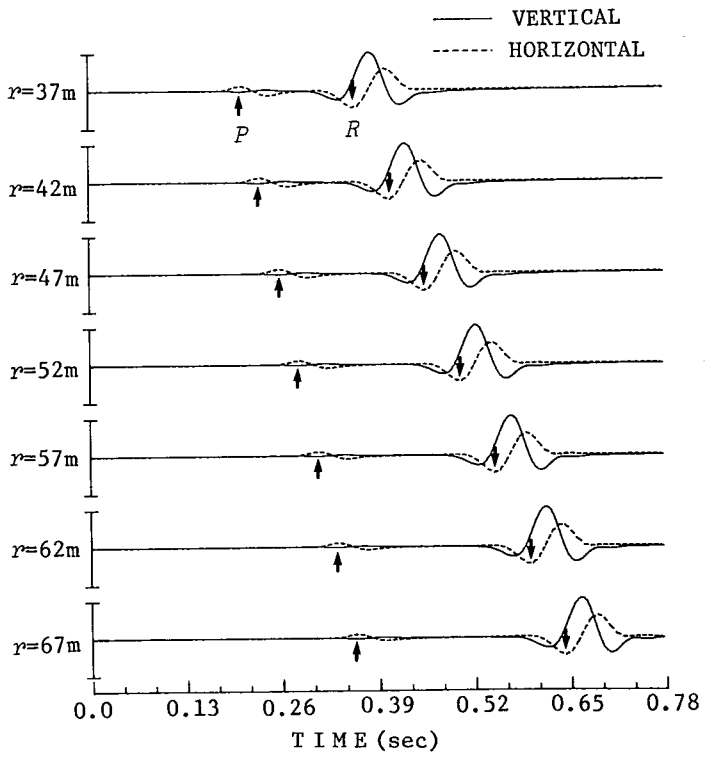


Fig.5. Vertical and Horizontal Displacement-Time Histories on the Surface of the Elastic Half-Space Model

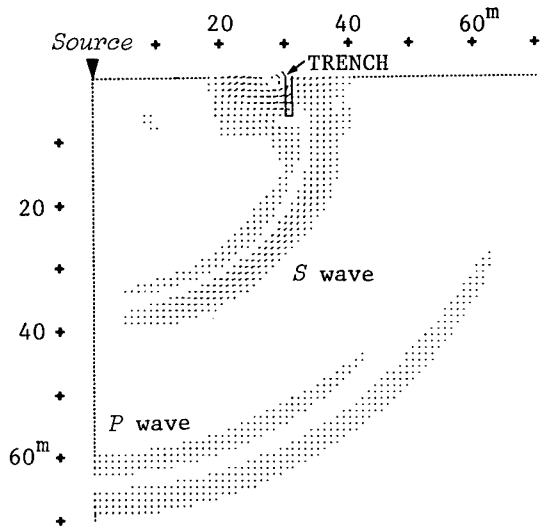


Fig.6. Displacement Vector Field in the Trench Model at $t=85\cdot\Delta t(L=3, D=0.6)$

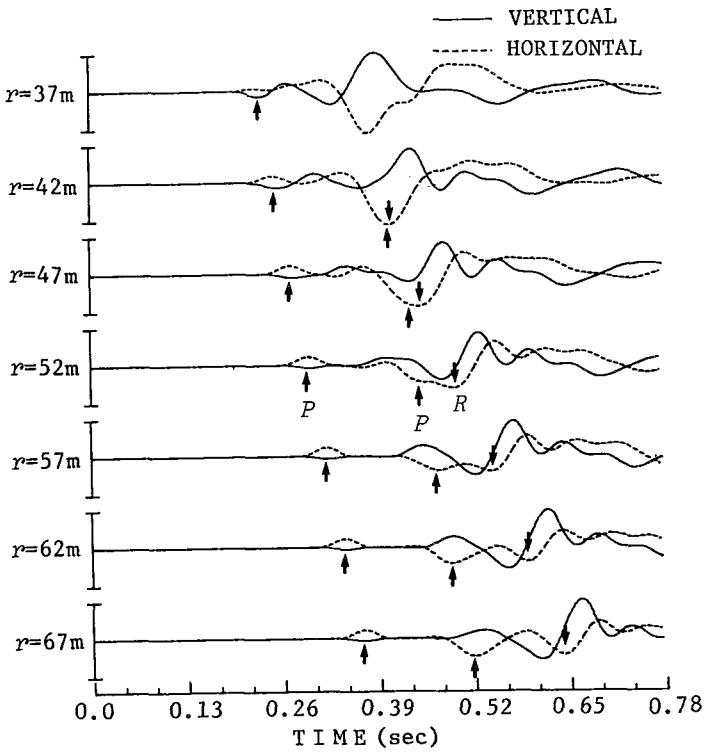


Fig.7. Vertical and Horizontal Displacement-Time Histories on the Surface of the Trench Model

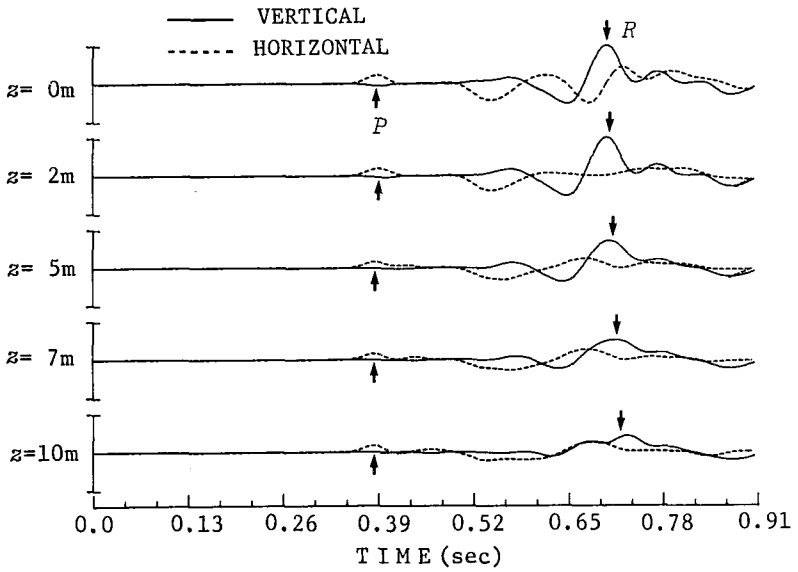


Fig.8. Vertical and Horizontal Displacement-Time Histories at Several Depths ($r$=70m) in the Trench Model

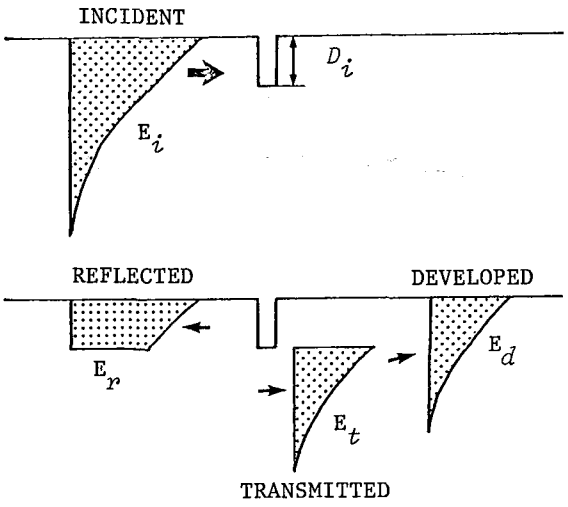


Fig.9. Schematic Illustration of Energy Partition of Incident Surface Wave into the Reflected, Transmitted and Developed Surface Wave at a Trench

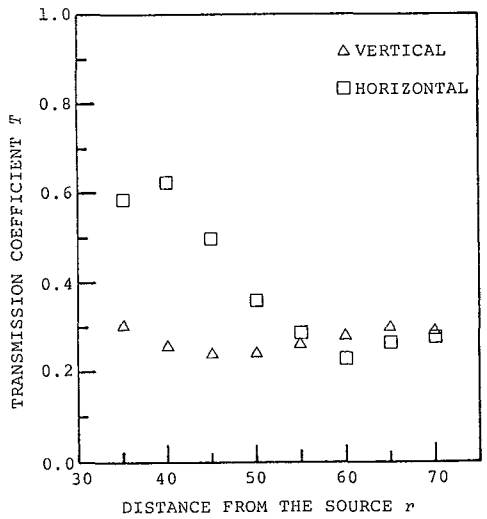


Fig.10. Relation between Transmission Coefficients and the Distance from the Source ($L$=3, $D$=0.6)

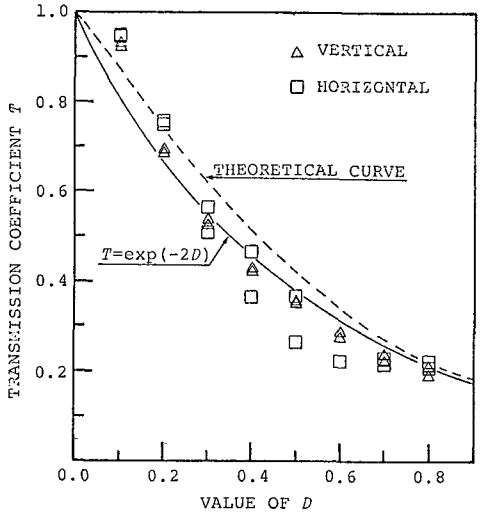


Fig.11. Relation between Transmission Coefficients in Far Field and the Value of $D$